Nanomagnetics

Numerical Ferromagnetic Resonance Experiments in Nanosized Elements

Kai Wagner[1,2], Lukas Körber[1,3], Sven Stienen[1,2], Jürgen Lindner[1], Michael Farle[2], and Attila Kákay[1]

[1] *Helmholtz-Zentrum Dresden-Rossendorf, Institute of Ion Beam Physics and Materials Research, 01328 Dresden, Germany*
[2] *Faculty of Physics and the Center for Nanointegration, University of Duisburg-Essen, 47057 Duisburg, Germany*
[3] *Fakultät Physik, Technische Universität Dresden, D-01062 Dresden, Germany*
[*] *Member, IEEE*

Received 12 Oct 2020, revised 2 Dec 2020, accepted 6 Dec 2020, published 29 Jan 2021, current version 31 Mar 2021.

Abstract—In this letter, we present a numerical approach to obtain the ferromagnetic resonance spectra of micrometer- and nanometer-sized magnetic elements by micromagnetic simulations. By mimicking common experimental conditions, we applied a static magnetic field and used a linearly polarized oscillating magnetic field to excite magnetization dynamics. A continuous single-frequency excitation is utilized, which permits the study of the steady-state dynamics in the space and time domain. This gives direct access to resonance fields, linewidths, and relative amplitudes as observed in the experiments, which is not easily accessible in pulsed schemes and allows for a one-to-one identification between simulation and experiment. Similar to numerical approaches using pulsed excitations, the phases, ellipticity, and spatial mode profiles of the spin-wave excitations may also be accessed. Using large excitation powers, we then showcase that one can additionally study nonlinear responses by this method, such as the nonlinear shift of the resonance fields and the foldover of the absorption lines. Since the dynamic susceptibility is directly determined from standard outputs of common micromagnetic codes, the presented method is robust, efficient, and easy-to-use, adding to its practical importance.

Index Terms—Nanomagnetics, ferromagnetic resonance, micromagnetic simulations, line width, nonlinear, foldover.

I. INTRODUCTION

The detailed understanding of spin-wave spectra of magnetic micro- and nanostructures and their magnetization dynamics has found increasing interest from both fundamental and application points of view, for example, in spin caloritronics and spin-torque phenomena [Kruglyak 2010, Lenk 2011, Madami 2011, Bauer 2012, Pile 2020]. A powerful tool to experimentally investigate spin-wave spectra with high spectral resolution is the ferromagnetic resonance (**FMR**), either detected directly in the frequency domain or in the field-swept mode at constant excitation frequency [Lindner 2008, Farle 2013]. However, in most cases, the measured FMR spectra are complex in nature, featuring several—often overlapping—resonances and require theoretical models of the nanostructured magnetic systems to extract quantitative information. Micromagnetic simulations of the FMR can be used to model such systems to provide information on the observed magnetic excitations, such as their character and dependence on magnetic parameters, geometries, or charge currents [McMichael 2006, Venkat 2013]. The micromagnetic approach is especially advantageous in case of complex geometries or interactions of nanoscale ferromagnets, when quantitative analytic approaches are not available.

Here, we present a numerical methodology to calculate the FMR of micrometer- and nanosized magnetic elements by micromagnetic simulations. In order to closely mimic the experimental conditions of continuous-wave excited FMR detection, we use an alternative approach to the common field-pulse excitation scheme. In addition to a static magnetic field, a single-frequency linearly polarized oscillating magnetic field is used to excite magnetization dynamics. As soon as the dynamic equilibrium is reached, the observed spin-wave excitations can be analyzed in the space and time domain. We show the relation between the volume-averaged magnetization dynamics and the complex dynamic susceptibility tensor. With our approach, one obtains not only information about the resonance fields, but also the otherwise difficult-to-obtain accurate linewidths, relative intensities, ellipticity of the magnetization precession, and phase relations of the excited spin-wave modes in the observed spectrum. These simulated parameters can be directly compared to the experimental data in a straightforward manner. The FMR spectra for large-amplitude microwave fields with its usual characteristics as the nonlinear frequency shift of the resonance fields or the foldover of the absorption curves can also be calculated, which is not accessible with the commonly used field-pulse excitation method. The spatially resolved magnetic response, plotted as a function of the external magnetic field and excitation frequency, yields a direct and detailed visualization of the spin-wave modes and their localization to different regions of the micromagnetic samples.

Corresponding author: Kai Wagner (e-mail: kai.wagner@unibas.ch).
Digital Object Identifier 10.1109/LMAG.2021.3055447

II. THEORETICAL BACKGROUND

Within the continuum limit, the dynamics of the magnetization vector field $\boldsymbol{M}(\boldsymbol{r}, t)$ in a ferromagnetic body is described by the Landau–Lifshitz–Gilbert (**LLG**) equation of motion [Gurevich 1996, Stancil 2009]

$$\frac{1}{\gamma}\frac{\mathrm{d}\boldsymbol{M}}{\mathrm{d}t} = -(\boldsymbol{M} \times \boldsymbol{H}_{\mathrm{eff}}) + \frac{\alpha}{M_{\mathrm{s}}}\left(\boldsymbol{M} \times \frac{\mathrm{d}\boldsymbol{M}}{\mathrm{d}t}\right) \tag{1}$$

where $\boldsymbol{H}_{\mathrm{eff}}$ is the effective field comprising the exchange, dipole–dipole, anisotropy, and external magnetic fields, M_{s} is the saturation magnetization, γ is the gyromagnetic ratio of the electron, and α is

the Gilbert-damping parameter. In case the magnetization is deflected away from its equilibrium, e.g., by an external magnetic field, a precession around the effective field occurs. By separating the magnetization into a static and a dynamic part $\boldsymbol{M}(\boldsymbol{r},t) = \boldsymbol{M}_{\rm eq}(\boldsymbol{r}) + \boldsymbol{m}(\boldsymbol{r},t)$, one can linearize (1) with respect to small-amplitude dynamic excitations $\boldsymbol{m}(\boldsymbol{r},t)$. As a result, the high-frequency response of a magnetic system to an external microwave **(RF)** field $\tilde{\boldsymbol{h}}_{\mathbf{RF}}$ can be expressed using the Polder susceptibility tensor $\hat{\chi}(\omega)$ as

$$\tilde{\boldsymbol{m}}(\boldsymbol{r},t) = \hat{\chi}(\omega)\cdot\tilde{\boldsymbol{h}}_{\rm RF}(\boldsymbol{r},t). \tag{2}$$

Here, we use the complex-amplitude notation such that the real parts $\boldsymbol{m} = \Re(\tilde{\boldsymbol{m}})$ and $\boldsymbol{h}_{\rm RF} = \Re(\tilde{\boldsymbol{h}}_{\rm RF})$ correspond to the respective physical observables. The Polder tensor $\hat{\chi}$, also referred to as dynamic susceptibility or high-frequency magnetic susceptibility, is a superposition of susceptibilities of the individual spin-wave modes and describes their linear response to an external driving field, i.e., their resonance frequencies and linewidths. The susceptibility may be split into a real and an imaginary part, $\hat{\chi} = \hat{\chi}' + i\hat{\chi}''$. In the case of a spatially homogeneous microwave field, the average power P absorbed by the magnetic system is proportional to the imaginary part of the Polder tensor [Vonsovskij 1966]

$$P(\omega) \propto \langle \tilde{\boldsymbol{h}}^{*}_{\rm RF}\cdot\hat{\chi}''(\omega)\cdot\tilde{\boldsymbol{h}}_{\rm RF}\rangle. \tag{3}$$

Here, $\langle\ldots\rangle$ denotes the spatial average in the sample volume, and the asterisk denotes the complex conjugate. As the signal measured in a conventional cavity-based FMR experiment is proportional to the average absorbed microwave power, the problem of simulating an FMR spectrum comes down to obtaining the necessary matrix elements of the imaginary part of the dynamic susceptibility $\hat{\chi}''$. Note that the resonance frequencies generally are dependent on the applied bias magnetic fields. In typical FMR experiments, the frequency of the microwave field is kept constant, and the static external field is varied. We may therefore consider the absorbed power as a function of static external field $P(H)$.

III. METHOD

In micromagnetic simulations, which rely on numerically solving a discretized version of the equation of motion (1), the *modus operandi* to calculate the spectrum of the modes susceptible to a microwave field with a certain spatial profile is a pulsed excitation scheme. A short magnetic field pulse of $\mathrm{sinc}(\omega_c t) = \sin(\omega_c t)/(\omega_c t)$ time dependence is applied followed by a Fourier transform of the time-dependent magnetization dynamics. The latter can be done on the average magnetization components or individually on the magnetization of all discretization cells. Although this method allows to quickly obtain the linear resonance frequencies and spatial profiles of the excitable modes below a certain cutoff frequency ω_c, it does not provide correct frequency linewidths, phases, or relative amplitudes, as measured in FMR experiments. Moreover, the simultaneous and short-timed excitation of different Fourier components does not lead to steady-state dynamics and prohibits to study equilibrium nonlinear dynamics and related energy flow. The method presented here is free of these shortcomings.

Generally speaking, our approach is much better adapted to replicate the conditions of conventional FMR experiments. A homogeneous external microwave field is applied and set to a fixed frequency, and an additional static external field is slowly varied stepwise within a certain range. For each field step, the microwave absorption is calculated based on (3), as will be explained in the following example. Whenever the field-dependent resonance frequencies match the frequency of the external microwave field, a local maximum in the power absorption, i.e., in the imaginary part of the dynamic susceptibility, is observed.

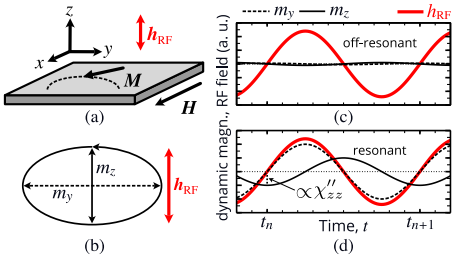

Fig. 1. Time-dependent response of the dynamic magnetization driven by an external RF field $\boldsymbol{h}_{\rm RF}$ for an infinite thin film magnetized in the xy-plane, as sketched in (a). The static field $\boldsymbol{H}$ is oriented in the film plane (x-direction) and is chosen to match the resonance condition. (b) Ellipticity of the magnetization dynamics can be determined from the dynamic components of the magnetization. The normalized dynamic magnetization components (solid and dashed black lines) in the yz-plane are shown together with the amplitude of the RF field $\boldsymbol{h}_{\rm RF}$ (red line) oriented along the film-normal in the z-direction along one period of excitation for the (c) off-resonance and (d) resonance cases. As marked in (d), the imaginary part of the susceptibility χ''_{zz} is proportional to the averaged out-of-plane component of the magnetization at the point when the RF field is crossing the zero value.

As an example, we consider a thin magnetic element, oriented in the xy-plane [see Fig. 1(a)]. The static external field is set to a chosen maximum value $H_{\rm max}$ and oriented in the x-direction. The static equilibrium magnetization $\boldsymbol{M}_{\rm eq}$ is then found either by minimizing the torque given by (1) or by minimizing the total magnetic energy. To excite the magnetization dynamics, the direction of the spatially homogeneous linearly polarized microwave field $\boldsymbol{h}_0\sin(\omega t)$ at fixed angular frequency ω is chosen along the out-of-plane (z) direction. Following (3), the absorbed microwave power is for this particular choice of geometry proportional to the imaginary part of the diagonal matrix element χ''_{zz}.

After an initial transient time, the torque exerted by the microwave field on the magnetization compensates the natural magnetic damping mechanisms and leads to stable forced oscillations in the dynamical components m_y and m_z at the angular frequency ω. Typically, in thin in-plane magnetized elements, the magnetic precession trajectory is elliptical due to the influence of the dipolar interaction, as seen in Fig. 1(b). To account for the initial transient phase, the magnetization is allowed to evolve for an integer number of time periods, $t_n = 2\pi\cdot n/\omega$, where n is chosen to provide a constant precession amplitude between consecutive oscillation cycles of the magnetization with a deviation of less than 0.02%. This number n typically depends on the magnetic parameters (e.g., damping constant α) and on the micromagnetic solver at hand. In Fig. 1(c) and (d), we show such a precession of the dynamical magnetization together with the microwave field for the off-resonant and resonant cases. As seen, at resonance, the component parallel to the microwave field m_z has a phase shift of $\pi/2$ with respect to the field, i.e., it has a local minimum when the field crosses zero at

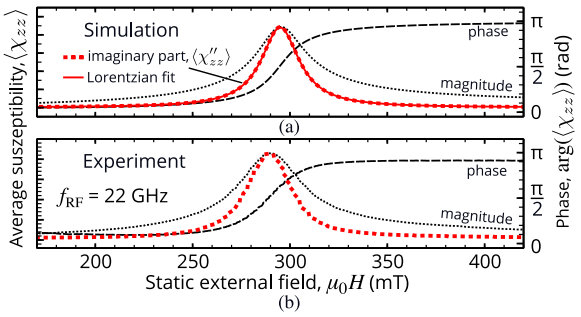

Fig. 2. (a) Micromagnetic simulation of the imaginary part, phase and magnitude of the average Polder susceptibility for an infinite thin film of 10 nm thickness. A fixed microwave frequency of 22 GHz is applied while the static magnetic field was swept stepwise downward. The material parameters are typical parameters for thin-film cobalt with $M_s = 1230\ \mathrm{kAm^{-1}}$, $\gamma/2\pi = 29.8\ \mathrm{GHz\ T^{-1}}$, and a slightly increased damping $\alpha = 0.016$ to account for material inhomogeneities. The magnetic resonance exhibits the classical hallmarks of a driven oscillator, where the oscillation magnitude has positive skew with respect to the external field. The imaginary part is a Lorentzian curve proportional to the experimentally detected FMR signal shown in (b). The resonance field of the experiment is different to the simulation, because the value of the saturation magnetization used in the numerics is only an effective value, which was obtained by fitting the well-known Kittel formula to the experimental data, neglecting crystal anisotropy [Gurevich 1996].

t_n. By inserting the sampling time t_n (periods of the RF field) into (2), taking the observable real part and averaging for the sample volume, the microwave-absorption power reads as

$$P \propto \langle\chi''_{zz}\rangle = -\frac{\langle m_z(t_n)\rangle}{h_0} \tag{4}$$

with $h_0 = |\boldsymbol{h}_0|$ being the modulus of the RF amplitude. Hence, by directly monitoring the average dynamical component $\langle m_z\rangle$ parallel to the microwave field $\boldsymbol{h}_{RF}$, an absorption proportional to the FMR signal can be obtained numerically, without further postprocessing. By a similar logic, the real part of the average susceptibility $\langle\chi'_{zz}\rangle$—and therefore the complete $\langle\chi_{zz}\rangle$—can be retrieved from the simulation by extracting $\langle m_z\rangle$ at the maximum of the microwave field, i.e., at $t_{n+1/4}$. This makes the presented method extremely efficient and practical, especially since the spatially averaged magnetization is provided by default by most micromagnetic codes. The field-dependent absorption curve $P(H)$ is obtained by incrementally decreasing the magnitude of the static external field H in small steps and repeating the procedure described earlier for each field step.

As seen in Fig. 2(a), the magnetic response (represented by the average matrix element $\langle\chi''_{zz}\rangle$) shows the typical hallmarks of a driven oscillator with respect to phase and magnitude. The imaginary part is a perfect Lorentzian absorption curve [Poole 1983]. This allows the determination of the resonance positions as well as their linewidth and relative signal strength. We compare the results to an experimentally obtained absorption curve for the example of a 10 nm thick Co film in Fig. 2(b), showing an excellent agreement with the simulation. The experimental curve was obtained using a coplanar waveguide (**CPW**) FMR setup [Körner 2013].

In the case of multiple superimposed resonances, a decomposition of the resultant spectra (experiment or simulation) into Lorentzian absorption lines is needed to obtain those quantities. The simulated spectra can be directly compared to complex experimental results, for example, for the case of micrometer-sized magnetic stripes [Banholzer 2011, Duan 2014, Schppner 2014]. Next to these spectra, one can additionally extract the spatial profile of the resonant spin-wave modes by considering the magnetization $\boldsymbol{M}(\boldsymbol{r}, t_n)$ of each cell. Moreover, in most cases, the average precession ellipticity can be obtained by sampling the average dynamical components ($\langle m_{y,z}\rangle$) for a large number of points within an additional period $[t_n, t_{n+1}]$.

IV. APPLICATIONS

To showcase this method, we use a custom version of the GPU-accelerated micromagnetic code MuMax^3 [Vansteenkiste 2014, Kakay 2021], which solves the LLG equation of motion (1) on a cuboid grid. However, we would like to note that the numerical FMR method presented here is completely independent of the micromagnetic code at hand. Alternatives include OOMMF [2006], TetraMag [Kákay 2010], NMAG-FinMag-Finimag [Fangohr 2002], and LLG Micromagnetic Simulator [Scheinfein 1997], among others. Of course, this method could also be used for simple macrospin simulations.

A. Characterizing the Linear Excitations in a Magnetic Element

As a first example, we characterize the magnetic excitations observable in FMR experiments in a 5.1µm ×1.1µm × 50 nm stripe made of permalloy (Ni_{80} Fe_{20}). For the material properties, we adopt typical values of the exchange constant $A_{ex} = 13\ \mathrm{pJm^{-1}}$, saturation magnetization $M_s = 790\ \mathrm{kAm^{-1}}$, reduced gyromagnetic ratio $\gamma/2\pi = 29.67\ \mathrm{GHz\ T^{-1}}$, and Gilbert-damping parameter $\alpha = 0.006$. Moreover, to mimic experimental conditions, the static external field is slightly tilted in-plane by a 0.5° angle toward the short axis of the stripe. The number of periods n before sampling the magnetization is set to 130. For codes based on double precision, e.g., OOMMF, this number can be smaller. The numerically obtained microwave absorption, together with the stripe geometry and field orientations is shown in Fig. 3(a).

In such a confined system, multiple magnetic resonances (in this case 3, labeled from 1 to 3) with differing resonance field positions, linewidths, and intensities occur [Hillebrands 2002]. The spatial distribution of the out-of-plane component of the dynamic magnetization $m_z(t_n)$ is shown for the two most intense resonances in Fig. 3(c) and (d). As discussed in Section III, these mode profiles are the natural outcomes of this continuous-wave excitation method. In Fig. 3(b), we compare the numerically obtained absorption curve to an experimental resonance line obtained from a real sample with the same dimensions and parameters, using a microresonator cavity. In contrast to the CPW-FMR technique, a single ferromagnetic object can be measured with a microresonator [Banholzer 2011, Schppner 2014, Schaffers 2017]. Since, in the experiments, the microwave absorption was measured using a lock-in technique, the derivative of both curves with respect to external field is shown. It can be seen that the experimental resonance fields are slightly different from the simulations, which are likely due to the fact that the saturation magnetization M_s and gyromagnetic ratio γ of the sample are not precisely known, as they were obtained from the FMR measurements. For better visual clarity, in Fig. 3(b), we only show the simulation data for the resonances observed in the experiments.

In the numerical FMR spectra [see Fig. 3(a)], the mode 1 exhibits the strongest excitation in the center of the stripe and will here be referred

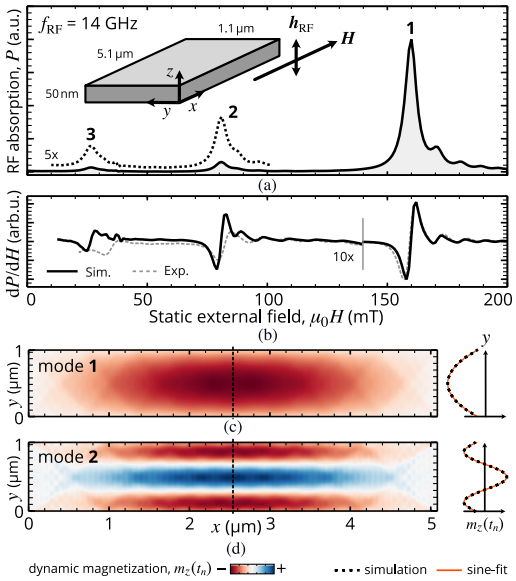

Fig. 3. (a) Micromagnetic simulation of the susceptibility χ''_{zz} for a 5.1 µm × 1.1 µm × 50 nm permalloy stripe and a fixed microwave frequency of 14 GHz. Multiple magnetic resonances are observed (labeled from 1 to 4). The derivative of the absorption curve is compared with an experimental curve in (b). The peaks are shifted probably due to a slightly different value of M_s in the simulations (see text). For clarity, the simulation data are only shown for the experimentally observed resonances. (c) and (d) Spatial profiles (out-of-plane component of the dynamic magnetization m_z at t_n) of the two lowest order modest together with line scans of m_z along the width of the stripe. The line scans were taken at the positions of the dashed lines.

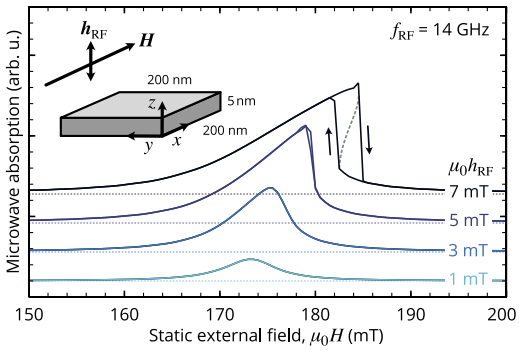

Fig. 4. Micromagnetic simulation of the field-dependent FMR of a 200 nm × 200 nm × 5 nm element made of permalloy for different amplitudes of the RF field. For better visualization, the curves are plotted with individual baselines indicated by the dotted horizontal lines. For the largest amplitude 7mT, a nonlinear foldover is seen, leading to hysteresis in the FMR when sweeping the static field in opposite directions. A dashed curve schematically indicates the theoretical shape of the foldover.

to as a localized quasi-uniform mode. A different mode character can be observed for the less intense mode 2. Its out-of-plane component shows a change in sign across the stripe, two nodal lines, and a wavelike varying dependence along the width of the stripe. Both modes can be very well approximated by a sinusoidal function, as shown in Fig. 3(c) and (d), and resemble the expected mode profile of a standing spin wave with wavelengths 2704 nm and 840 nm for modes 1 and 2, respectively. These wavelengths differ from the expected values for simply closed or open pinning conditions and are a result of the dipolar pinning at the edges of the stripe [Guslienko 2002]. In a similar consideration, resonances 3 and 4 can be assigned to higher order standing spin waves across the width of the stripe, where the wavelength decreases for smaller resonance fields.

By such a spatial analysis, one can, for example, explore the dependence of the microwave absorption spectra and magnetic excitations on the magnetic parameters as well as on the exact geometry of the magnetic systems. This information can be crucial for planning experiments and deeper understanding of the possibly large number of resonances in experimentally observed spectra, e.g., as also performed in Banholzer [2011]. Furthermore, this method can also be used to study traveling modes [Pile 2020], dynamics in complex structures, as shown for magnetic nanotubes [Lenz 2019], or (by also varying the microwave frequency) to obtain the full field-frequency-dependent microwave absorption of a given sample.

B. Nonlinear FMR

As a second example, we show that the method can also be employed to qualitatively study weakly nonlinear dynamics, i.e., the nonlinear FMR. As first observed by Bloembergen [1952], Damon [1953], and Bloembergen [1954] and described by Suhl [1957], the spin-wave modes observed in FMR experiments become unstable above a certain amplitude of the microwave field $\boldsymbol{h}_{RF}$. Such phenomena are historically referred to as Suhl instabilities and are typically related to three- or four-wave scattering processes. They result in a RF-power-dependent nonlinear shift of the resonance frequencies, a broadening of the linewidths, and, ultimately, in a foldover of the absorption curves. Note that this example is a perturbative extension of the earlier analysis showcase toward large driving amplitudes, since strictly speaking, the Polder susceptibility has been introduced for the linear regime. At very large driving powers, for example, higher harmonic contributions may appear and, in particular, oscillations in the dynamical component parallel to the static external field have to be taken into account. However, at intermediate powers, when the nonlinear dynamic equilibrium is reached, the oscillation modes remain often well-described as being proportional to $\exp(-i\omega_{NL}t)$ (with ω_{NL} being a power-dependent resonance frequency), and the same arguments as the ones used in Section III can be made in an approximate manner to derive the microwave absorption.

To showcase this, we consider a 200 nm × 200 nm × 5 nm element made of permalloy with exchange constant $A_{ex} = 13$ pJm^{-1}, saturation magnetization $M_s = 810$ kAm^{-1}, reduced gyromagnetic ratio $\gamma/2\pi = 29.81$ GHz T^{-1}, and Gilbert-damping parameter $\alpha = 0.007$. Fig. 4 shows a part of the numerical absorption curves for different amplitudes of the RF field. As expected for thin in-plane magnetized elements [Krivosik 2010], we observe a positive nonlinear shift of the resonance field and a consequential foldover, which leads to a region of bistability, i.e., a hysteresis in the absorption curves. Because of this hysteresis, the curves have been obtained for decreasing and increasing static external field as indicated by the schematic arrows. Note that the simulation of a field-step takes only half a minute (performed using MuMax^3 on a TITAN Xp GPU) and can be readily parallelized. A direct comparison with experimental data is cumbersome in this case and would go beyond the scope of this letter, as it requires sufficient knowledge of the microwave power arriving at the microwave antenna at hand. We would like to note that this method can also be extended to parallel-pumping FMR [Schlömann 1962, Venugopal 2020].

V. CONCLUSION

In summary, we presented a numerical method to calculate FMR spectra using micromagnetic simulations. The method utilizes a single-frequency continuous-wave magnetic field for excitation, which allows to study the steady-state equilibrium and extract the full field-dependent dynamical susceptibility in a straightforward manner. In contrast to common pulsed schemes, our method yields linewidths and relative intensities of spin-wave modes directly comparable to those measured in FMR experiments. This eases the direct cross-identification of observed resonances, in particular, for complex scenarios of nanosized magnetic elements. The steady-state FMR spectra and magnetic excitations are directly visualized based on the default outputs of common micromagnetic codes, which renders this method easy to use, efficient, and robust in postprocessing. In addition, we showed that the nonlinear magnetic response for large driving amplitudes, such as the nonlinear frequency shift of the resonance fields or the foldover of the absorption curves, can be studied.

This method may be extended to analyze the transient phase prior to a dynamic equilibrium and standing wave formation processes. Such dynamic processes may become of interest for magnetic samples in which simple standing spin-wave formation is modified by chiral symmetry breaking and interpretation of FMR spectra requires the aid of accurate modeling. We believe that with the recent development of high-performance micromagnetic codes, the method can be used as a powerful numerical method to corroborate FMR experiments and help interpret the experimentally obtained results.

ACKNOWLEDGMENT

This work was supported by the Deutsche Forschungsgemeinschaft (SFB 491, KA 5069/1-1, KA 5069/3-1, Project-ID 405553726—TRR 270). The work of Michael Farle was supported by the Government of the Russian Federation under Research Grant 075-15-2019-1886. The authors thank C. Hassel and R. Meckenstock.

REFERENCES

Banholzer A, Narkowicz R, Hassel C, Meckenstock R, Stienen S, Posth O, Suter D, Farle M, Lindner J (2011), "Visualization of spin dynamics in single nanosized magnetic elements," *Nanotechnology*, vol. 22, 295713, doi: 10.1088/0957-4484/22/29/295713.

Bauer G E W, Saitoh E, van Wees B J (2012), "Spin caloritronics," *Nat. Materials*, vol. 11, pp. 391–399, doi: 10.1038/nmat3301.

Bloembergen N, Damon R W (1952), "Relaxation effects in ferromagnetic resonance," *Phys. Rev.*, vol. 85, 699, doi: 10.1103/PhysRev.85.699.

Bloembergen N,Wang S (1954), "Relaxation effects in para- and ferromagnetic resonance," *Phys. Rev.*, vol. 93, pp. 72–83, doi: 10.1103/PhysRev.93.72.

Cansever H, Narkowicz R, Lenz K, Fowley C, Ramasubramanian L, Yildirim O, Niesen A, Huebner T, Reiss G, Lindner J, Fassbender J, Deac A M (2018), "Investigating spin-transfer torques induced by thermal gradients in magnetic tunnel junctions by using micro-cavity ferromagnetic resonance," *J. Phys. D: Appl. Phys.*, vol. 51, pp. 224009–224019, doi: 10.1088/1361-6463/aac03d.

Damon R W (1953), "Relaxation effects in the ferromagnetic resonance," *Rev. Modern Phys.*, vol. 25, pp. 239–245, doi: 10.1103/RevModPhys.25.239.

Donahue M J, Porter D G (2010), "OOMMF User's Guide, Version 1.2a3," Nat. Inst. Standards Technol., Gaithersburg, MD, USA.

Duan Z, Boone C T, Cheng X, Krivorotov I N, Reckers N, Stienen S, Farle M, Lindner J (2014), "Spin-wave modes in permalloy/platinum wires and tuning of the mode damping by spin Hall current," *Phys. Rev. B*, vol. 90, 0 24427, doi: 10.1103/PhysRevB.90.024427.

B. Marc-Antonio *et al.*, "FinMag: finite-element micromagnetic simulation tool," Apr. 2018. [Online]. Available: https://zenodo.org/record/1216011{\#}.XYDDMJMzb1I

Farle M, Silva T, Woltersdorf G (2013), "Spin dynamics in the time and frequency domain," in *Magnetic Nanostructures: Spin Dynamics and Spin Transport.* (ser. Springer Tracts in Modern Physics), Zabel H, Farle M, Eds., vol. 246. Berlin, Heidelberg: Springer Berlin Heidelberg, pp. 37–83, doi: 10.1007/978-3-642-32042-2_2.

Gurevich A G, Melkov G A (1996), *Magnetization Oscillations and Waves*. Boca Raton, FL, USA: CRC Press. [Online]. Available: https://www.crcpress.com/Magnetization-Oscillations-and-Waves/Gurevich-Melkov/p/book/9780849394607

Guslienko K Y, Demokritov S O, Hillebrands B, Slavin A N (2002), "Effective dipolar boundary conditions for dynamic magnetization in thin magnetic stripes," *Phys. Rev. B*, vol. 66, 132402, doi: 10.1103/PhysRevB.66.132402.

Hillebrands B (2002), *Spin Dynamics in Confined Magnetic Structures*. Berlin, Germany: Springer.

Kákay, A (2021), "Curvilinear micromagnetism," [Online]. Available: https://www.hzdr.de/db/Cms?pOid=55944&pNid=107

Kákay A, Westphal E, Hertel R (2010), "Speedup of FEM micromagnetic simulations with graphical processing units," *IEEE Trans. Magn.,* vol. 46, pp. 2303–2306, doi: 10.1109/TMAG.2010.2048016.

Kittel C (1948), "On the theory of ferromagnetic resonance absorption," *Phys. Rev*., vol. 73, pp. 155–161, doi: 10.1103/PhysRev.73.155.

Körner M, Lenz K, Gallardo R A, Fritzsche M, Mücklich A, Facsko S, Lindner J, Landeros P, Fassbender J (2013), "Two-magnon scattering in permalloy thin films due to rippled substrates," *Phys. Rev. B*, vol. 88, 0 54405, doi: 10.1103/PhysRevB.88.054405.

Krivosik P, Patton C E (2010), "Hamiltonian formulation of nonlinear spin-wave dynamics: Theory and applications," *Phys. Rev. B*, vol. 82, 184428, doi: 10.1103/PhysRevB.82.184428.

Kruglyak V V, Demokritov S O, Grundler D (2010), "Magnonics," *J. Phys. D: Appl. Phys*., vol. 43, 264001, doi: 10.1088/0022-3727/43/26/264001.

Landau L, Lifshits E (1935), "18 - on the theory of the dispersion of magnetic permeability in ferromagnetic bodies," *Collected Papers of L.D. Landau*, Editor, D. Ter Haar, Pergamon: vol. 8, pp. 101–114, 1965. [Online]. Available: https://www.sciencedirect.com/science/article/pii/B9780080105864500237

Lenk B, Ulrichs H, Garbs F, Münzenberg M (2011), "The building blocks of magnonics," *Phys. Rep.*, vol. 507, pp. 107–136, doi: 10.1016/j.physrep.2011.06.003.

Lenz K, Narkowicz R, Wagner K, Reiche C F, Körner J, Schneider T, Kákay A, Schultheiss H, Weissker U, Wolf D, Suter D, Büchner B, Fassbender J, Mühl T, Lindner J (2019), "Magnetization dynamics of an individual single-crystalline Fe-filled carbon nanotube," *Small*, vol. 15, 1904315, doi: 10.1002/smll.201904315.

Lindner J, Farle M (2008), "Magnetic anisotropy of heterostructures," in *Magnetic Heterostructures.* (ser. Springer Tracts in Modern Physics), vol. 227. Berlin, Germany: Springer, pp. 45–96.

Madami M, Bonetti S, Consolo G, Tacchi S, Carlotti G, Gubbiotti G, Mancoff F B, Yar M A, Åkerman J (2011), "Direct observation of a propagating spin wave induced by spin-transfer torque," *Nat. Nanotechnol.*, vol. 6, pp. 635–638, doi: 10.1038/nnano.2011.140.

McMichael R D, Maranville B B (2006), "Edge saturation fields and dynamic edge modes in ideal and nonideal magnetic film edges," *Phys. Rev. B*., vol. 74, 0 24424, doi: 10.1103/PhysRevB.74.024424.

OOMMF (2006), "The object oriented MicroMagnetic framework (OOMMF) project at ITL/NIST," [Online]. Available: https://www.hzdr.de/db/Cms?pOid=55944&pNid=107

Pile S , Feggeler T, Schaffers T, Meckenstock R, Buchner M, Spoddig D, Zingsem B, Ney V, Farle M, Wende H, Ohldag H, Ney A, Ollefs K (2020), "Non-standing spin-waves in confined micrometer-sized ferromagnetic structures under uniform excitation," *Appl. Phys. Lett.*, vol. 116, 0 72401, doi: 10.1063/1.5139881.

Poole C P (1983), *Electron Spin Resonance*. Hoboken, NJ, USA: Wiley.

Schaffers T, Meckenstock R, Spoddig D, Feggeler T, Ollefs K, Schöppner C, Bonetti S, Ohldag H, Farle M, Ney A (2017), "The combination of micro-resonators with spatially resolved ferromagnetic resonance," *Rev. Sci. Instrum*., vol. 88, 0 93703, doi: 10.1063/1.4996780.

Scheinfein M R (1997), *LLG Micromagnetics Simulator, Software for Micro-Magnetic Simulations*. [Online]. Available: https://llgmicro.home.mindspring.com/

Schlömann E (1962), "Longitudinal susceptibility of ferromagnets in strong RF fields," *J. Appl. Phys.*, vol. 33, pp. 527–534, doi: 10.1063/1.1702461.

Schoeppner C, Wagner K, Stienen S, Meckenstock R, Farle M, Narkowicz R, Suter D, *Lindner J (2014)*, "Angular dependent ferromagnetic resonance analysis in a single micron sized cobalt stripe," *J. Appl. Phys.*, vol. 116, 0 33913, doi: 10.1063/1.4890515.

Stancil D D, Prabhakar A (2009), *Spin Waves: Theory and Applications*. Berlin, Germany: Springer.

Suhl H (1957), "The theory of ferromagnetic resonance at high signal powers," *J. Phys. Chem. Solids*, vol. 1, pp. 209–227, doi: 10.1016/0022-3697(57)90010-0.

Vansteenkiste A, Leliaert J, Dvornik M, Helsen M, Garcia-Sanchez F, Van Waeyenberge B (2014), "The design and verification of MuMax3," *AIP Adv.*, vol. 4, 107133, doi: 10.1063/1.4899186.

Venkat G, Kumar D, Franchin M, Dmytriiev O, Mruczkiewicz M, Fangohr H, Barman A, Krawczyk M, Prabhakar A (2013), "Proposal for a standard micromagnetic problem: Spin wave dispersion in a magnonic waveguide," *IEEE Trans. Magn.*, vol. 49, pp. 524–529, doi: 10.1109/TMAG.2012.2206820.

Venugopal A, Qu T, Victora R H (2020), "Nonlinear parallel-pumped FMR: Three and four magnon processes," *IEEE Trans. Microw. Theory Techn.*, vol. 68, pp. 602–610, doi: 10.1109/TMTT.2019.2952128.

Vonsovskii S. V., "Ferromagnetic resonance; the phenomenon of resonant absorption of a high-frequency magnetic field in ferromagnetic substances," Edited, S.V. Vonsovski. Translated by H.S.H. Massey. Translation edited by D. ter Haar, New York, NY, USA: Pergamon. p. 325, 1966. [Online]. Available: https://nla.gov.au/nla.cat-vn4043